

Vertical magneto-tunneling through a quantum dot and the density of states of small electronic systems

Augusto Gonzalez^{a1,2} and Roberto Capote^{b3}

¹ Departamento de Fisica, Universidad de Antioquia, AA 1226, Medellin, Colombia

² Instituto de Cibernetica, Matematica y Fisica Calle E 309, Vedado, Habana 4, Cuba

³ Centro de Estudios Aplicados al Desarrollo Nuclear, Calle 30 No 502, Miramar,

La Habana, Cuba

(October 27, 2018)

One-electron tunneling through a quantum dot with a strong magnetic field in the direction of the current is studied. The linear magneto-conductance is computed for a model parabolic dot with seven electrons in the intermediate states and for different values of the magnetic field. It is shown that the dot density of states at low excitation energies can be extracted from a precise measurement of the conductance at the upper edge of the Coulomb blockade diamond. We parametrized the density of states with a single “temperature” parameter (in the so called “constant temperature approximation”), and found that this parameter depends very weakly on the magnetic field.

PACS number(s): 73.23.Hk, 73.21.La, 73.43.Jn

Keywords: Single-electron tunneling, density of levels, quantum dots, high magnetic fields

I. INTRODUCTION

The experimental study of vertical transport through a semiconductor quantum dot¹ have stressed the similarities of these small electronic systems with real atoms. Shell effects (in a confinement potential which is approximately parabolic in shape) and spin effects are clearly distinguished in the positions of conductance peaks². The inclusion of a relatively strong magnetic field, B , makes possible to measure spin reordering with B up to the formation of a completely polarized electronic droplet³. The technique has also revealed its power as a spectroscopic tool in the determination of the low-lying energy levels of the few-electron dots⁴. More recent developments include integer spin Kondo effects⁵, and the study of two-electron tunneling in the Coulomb blockade regime⁶.

The position of conductance peaks, obtained from the experiments, determine addition energies and even excitation energies to the first excited states, if they are well separated from the rest of the states. This only happens for the few-electron dots and for the very first excited states. In the six-electron dot, for example, at excitation energies around 1 meV, the density of states may be as high as 80 levels/meV. That is, mean level distance around 0.012 meV (see Section III). In the present paper, we show that for relatively small dots and excitation energies ≤ 1 meV, the density of states can be obtained from a precise measurement of the height and position of the conductance peak at the upper edges of the Coulomb blockade diamonds.

We present model calculations for a 6-electron dot in a magnetic field $8.75 \leq B \leq 12$ T. Our model parameters are chosen to approximate the experimental conditions in papers 3,6. The relatively strong magnetic field guarantees that only spin-polarized states are relevant in tunneling processes. On the other hand, the temperature is low enough (a few mK) for thermal excitation to be neglected. Thus a pure quantum mechanical description is used.

The plan of the paper is as follows. The details of the model quantum dot are specified in Section II. In the next section, the low-lying energy levels of the 6- and 7-electron dots are computed, and the density of levels at low excitation energies is parametrized with a single “temperature” parameter. We show that this parameter depends very weakly on the magnetic field. The calculation of the linear magneto-conductance (transmission coefficient) is sketched in Section IV. In Section V, we show how the conductance at maxima can be related to the density of energy levels, and we compare the estimate following from the conductance with the actual (calculated) density of states.

II. THE MODEL QUANTUM DOT

A schematic representation of the vertical profile (z axis) of the bottom of the conduction band for the model structure to be used is given in Fig. 1a. This is a symmetric AlGaAs(7 nm)-InGaAs(12 nm)-AlGaAs(7 nm) quantum well, with n-doped source (S) and drain (D) contacts⁶. The quantum dot is formed within the well region. For the smallest dots, the lateral (xy) confinement is approximately parabolic, with $\hbar\omega_0 = 3$ meV³.

The source potential will be taken as the reference potential. It will be fixed to zero. The barrier height due to the Al concentration is estimated in Ref. 6 as 50 meV. We will add 42 meV corresponding to the Coulomb barrier

(6 electrons times 7 meV). Thus, the top of the left barrier is at 92 meV, and for the right barrier at $(92 - V_{sd})$ meV (V_g and V_{sd} are in fact energies, not voltages). The drain potential is $-V_{sd}$. Notice that our V_g parameter is not the one used in experiments. In our model, the depth of the potential well is $-(V_g + V_{sd}/2)$, while in experiments V_g is related to the depth of the well through the capacitance of the system.

The electron mass and dielectric constant are taken as $0.067m_0$ and 12.5 respectively all over the structure. In the computation of the N -electron states in the dot, a first quantum well sub-band approximation is used. The energy of the first quantum well state, E_z , is computed numerically as a function of V_g and V_{sd} . The total energy is then written

$$E = NE_z + E_{xy}, \quad (1)$$

where E_{xy} is obtained from a two-dimensional calculation which includes the lateral confinement and the effective Coulomb potential (equal to 0.8 times the two-dimensional potential to account for averaging in the z direction).

Magnetic field values around 10 T are considered. In this region, the electronic droplet is completely spin polarized³. Moreover, the separation between Landau levels (LL) is $\hbar\omega_c = 1.728 B$ meV, where B is measured in Teslas. Thus, the second LL is around 17 meV above the first. If we are interested in excitation energies below 1 meV, we may neglect contributions from the second and higher LL's⁷. In section III, a large basis of Slater first LL functions is used to construct the two-dimensional matrix hamiltonian, which is further diagonalized by means of a Lanczos algorithm.

In section IV, we will compute the transmission coefficient of the model shown in Fig. 1, in which the potential is sectionally constant, unlike a real structure.

III. DENSITY OF LEVELS AT LOW EXCITATION ENERGIES

In the present section, we show results for the spin-polarized energy levels of the 6- and 7-electron dots. The starting point is the “first LL” H_{xy} hamiltonian

$$H_{xy} = (|M| + N)\hbar\Omega - |M|\hbar\omega_c/2 + \beta \sum_{i,j,k,l} < i, j | 1/r | k, l > a_i^+ a_j^+ a_l a_k, \quad (2)$$

where $\omega_c = eB/(mc)$ is the cyclotronic frequency, and $\Omega = \sqrt{\omega_0^2 + (\hbar\omega_c/2)^2}$. The sum runs over indexes, l , representing angular momentum projection onto the z axis. a_l^+ creates one electron in a harmonic oscillator state of frequency Ω with zero radial quantum number and $l \leq 0$. The Zeeman energy is not included. The constant β equals $0.8 e^2/(\kappa l_\Omega)$, where l_Ω is the harmonic oscillator length, and κ – the dielectric constant.

The hamiltonian H_{xy} is diagonalized in a basis of Slater determinants with fixed angular momentum projection $M = \sum_{t=1}^N l_t$. For a given M , this basis is finite. In a 7-electron system, for example, the sector with $M = -80$ contains 40340 functions. These large matrices are better diagonalized with a Lanczos algorithm.

We show in Fig. 2 the lowest energy levels (excitation energy ≤ 1 meV) for the $N = 6$ and 7-electron dots in magnetic fields $B = 8.75$ and 12 T. A few remarkable facts are evident from this figure. The average number of levels, n , with excitation energies $\leq \Delta E$ may be very well fitted by a “constant temperature approximation”⁸

$$n = \exp(\Delta E/\Theta). \quad (3)$$

The temperature parameter, Θ , exhibits a weak dependence on the magnetic field. When B varies from 8.75 to 12 T, for example, $1/\Theta$ for the 6-electron dot changes only from 2.99 to 3.20 (meV)⁻¹. In the language of “filling factors”, $\nu \approx M_0/M_{gs}$ (where $M_0 = -N(N-1)/2$ is the momentum corresponding to filling factor one), one has $\nu = 15/35 = 3/7$ at $B = 8.75$ T, and $\nu = 15/45 = 1/3$ for $B = 12$ T. The gap to the first excited state shrinks to zero at the B values where the ground-state momentum, M_{gs} , changes first from -35 to -39, and then from -39 to -45. Θ , however, varies very weakly. It means that Θ is not a measure of this gap, but of the actual low-lying density of levels.

The average density of levels following from Eq. (3) is

$$\frac{dn}{dE} = \frac{1}{\Theta} \exp(\Delta E/\Theta), \quad (4)$$

which may be taken as a smooth version of the actual density

$$\frac{dn}{dE} = \sum_r \delta(\Delta E - \Delta E_r), \quad (5)$$

where ΔE_r denotes the excitation energy of the r -th level. For $N = 6$ and $B = 12$ T, for example, the average density is around 80 levels/meV at $\Delta E = 1$ meV.

IV. LINEAR MAGNETO-CONDUCTANCE

We will compute the conductance, dI/dV_{sd} , from the transmission coefficient, T , by means of a simplified Landauer expression⁹

$$\frac{dI}{dV_{sd}} = \frac{e^2}{h} T. \quad (6)$$

Only one spin polarization is considered in (6) due to the quenching of the spin-down states by the magnetic field. T is computed from the usual relation between transmitted and incident current in the z direction.

The fact that there is only one electron tunneling through the structure allows one to write an ansatz for the total wave function in which N electrons are permanently confined inside the dot. We restrict our attention to 6 confined, and a seventh tunneling electron. Thus, we shall work in the interval of V_g values corresponding to the N=6 Coulomb blockade diamond of Fig. 1b. We shall focus on the first conductance peak when V_{sd} is varied, i. e. the edge of the diamond.

As mentioned above, only spin polarized states are considered. The reason is the following. Initial states for the tunneling processes are states with N electrons in the dot and one free electron in the source electrode. The energy is given in Eq. (9). Contributions to the transmission coefficient come from intermediate states of $N + 1$ electrons in the dot, and final states with N electrons in the dot and one electron in the drain, which energy is less or equal than the energy given in Eq. (9). As we are interested in the first conductance peak when V_{sd} is increased, only one intermediate state contributes, i. e. the ground state of $N + 1$ electrons in the dot. In a strong magnetic field, this is a spin polarized state. The long spin-relaxation times in quantum dots due to phase space reduction^{10,11}, make spin-flip processes in the final stage of tunneling impossible. Thus, relevant final states are also spin polarized.

The total wave function is written in a separable way: $\Psi = \Psi_z \Psi_{xy}$. The ansatz for the z function is the following:

$$\Psi_z = \chi(z_7) \prod_{u=1}^6 \chi_1(z_u), \quad (7)$$

where χ_1 is the first quantum well function. We will determine the combination $\chi(z_7)\Psi_{xy}$ in each z interval where the z -potential is sectionally constant. For Ψ_{xy} , a Fock representation will be used. We will simplify the notation further, writing $|\alpha\rangle$ instead of $\Psi_{xy}(N)$, and $|\gamma\rangle$ instead of $\Psi_{xy}(N+1)$. $|\alpha_0\rangle$ will denote the ground state. Then, the ansatz for the wave function is the following

(1) $z < 0$:

$$\Psi_1 = \hat{a}_{l_0}^\dagger |\alpha_0\rangle \{ \exp ik_1 z + b_1 \exp -ik_1 z \}, \quad (8)$$

where $k_1 = \sqrt{2m\epsilon_1}/\hbar$, and the total energy is written (apart from trivial constants) as

$$E = E_{\alpha_0} + \frac{\hbar\omega_c}{2} + \epsilon_1. \quad (9)$$

ϵ_1 is the initial kinetic energy of the tunneling electron. We will fix it at a small value, $\epsilon_1 = 0.01$ meV. $\hat{a}_{l_0}^\dagger$ is the (xy) creation operator for an electron with angular momentum projection l_0 in S. Due to the assumed cylindrical symmetry, the total angular momentum, $M = M_{\alpha_0} + l_0$ is a conserved quantity.

(2) $0 < z < L_B$:

$$\Psi_2 = \hat{a}_{l_0}^\dagger |\alpha_0\rangle \{ a_2 \exp -k_2 z + b_2 \exp k_2 z \}, \quad (10)$$

where $\epsilon_2 = \epsilon_1$, and $k_2 = \sqrt{2m(V_B - \epsilon_2)}/\hbar$. $V_B = 92$ meV is the barrier height.

(3) $L_B < z < L_B + L$:

$$\Psi_3 = \sum_\gamma |\gamma\rangle \{ a_3^\gamma \exp ik_3^\gamma z + b_3^\gamma \exp -ik_3^\gamma z \}, \quad (11)$$

where $k_3^\gamma = \sqrt{2m(V_g + V_{sd}/2 + \epsilon_3^\gamma)}/\hbar$, and $\epsilon_3^\gamma = \epsilon_1 + E_{\alpha_0} + \hbar\omega_c/2 - E_\gamma$.

(4) $L_B + L < z < 2L_B + L$:

$$\Psi_4 = \sum_\alpha \hat{a}_{l_\alpha}^\dagger |\alpha\rangle \{ a_4^\alpha \exp -k_4^\alpha z + b_4^\alpha \exp k_4^\alpha z \}, \quad (12)$$

where $k_4^\alpha = \sqrt{2m(V_B - V_{sd} - \epsilon_4^\alpha)}/\hbar$, and $\epsilon_4^\alpha = \epsilon_1 + E_{\alpha_0} - E_\alpha$. Finally,
(5) $2L_B + L < z$:

$$\Psi_5 = \sum_\alpha \hat{a}_{l_\alpha}^\dagger |\alpha\rangle a_5^\alpha \exp ik_5^\alpha z, \quad (13)$$

where $\epsilon_5^\alpha = \epsilon_4^\alpha$, and $k_5^\alpha = \sqrt{2m(V_{sd} + \epsilon_5^\alpha)}/\hbar$. The sum in (13) runs over open final state channels, i. e.

$$E_\alpha < \epsilon_1 + E_{\alpha_0} + V_{sd}. \quad (14)$$

In the above formulae, $L_B = 7$ nm and $L = 12$ nm are the barrier and well widths respectively. Notice that our ansatz for Ψ respects a weak version of the Pauli principle, but it is not completely antisymmetrized with respect to the seventh electron.

The continuity of the current leads to relations among the coefficients a and b in the different regions. With our ansatz, however, we found impossible to satisfy the continuity relations for general linear combinations of intermediate or final states. It means that we shall compute the transmission coefficient for each pair (γ, α) independently. We will refer to the pair (γ, α) as a tunneling channel. We will be particularly interested in the (γ_0, α) channels, where the intermediate state is the ground state of $N + 1$ electrons in the dot. The upper edge of the $N = 6$ Coulomb blockade diamond in Fig. 1b is related to these channels. Notice that the absence of interference between tunneling channels should be further reinforced by temperature effects. Note also that overlapping coefficients of transversal (x, y) functions cancel out in ratios b/a , and thus in T .

The partial transmission coefficient, T_α is defined as usual

$$T_\alpha = I_D(\alpha)/I_S, \quad (15)$$

where I_S is the incident current, and $I_D(\alpha)$ is the transmitted current when only the α channel is considered open. The total transmission coefficient is obtained from charge conservation arguments. If there are a few open channels, then $I_S T_1$ is the current flowing through channel 1, $I_S(1 - T_1)T_2$ is the current through channel 2, etc. The total coefficient is then

$$T = 1 - \prod_{\text{open channels}} (1 - T_\alpha). \quad (16)$$

V. RESULTS AND DISCUSSION

We show in Fig. 3a the partial transmission coefficient, T_2 corresponding to the excited state $\alpha = 2$ at excitation energy $\Delta E_2 = 0.425$ meV in a magnetic field $B = 12$ T. This channel is closed for $V_{sd} < 0.42$ meV, as expected. Three situations are depicted: below resonance ($V_g = 39.89$ meV), maximum resonance ($V_g = 39.87$ meV), and above resonance ($V_g = 39.6$ meV). The asymptotic shape of the curve below resonance is typical. In Nuclear Physics context, it is interpreted as interference between resonance and potential scattering¹². The maximum resonance occurs at a V_{sd} slightly higher than ΔE_2 . Note that, as the incident electron energy is fixed, the maximum of T_2 is not one, but a value around 0.85. Above resonance, the $\alpha = 2$ channel remains open but the transmission coefficient diminishes.

The computation of T from Eq. (16) show results like the one drawn in Fig. 3b, where all of the open channels (γ, α) at a given V_{sd} are included. V_g is 39.89 meV, and $B = 12$ T. The distance between the two peaks, 0.6 meV, is approximately twice the excitation energy to the first excited state of $N + 1$ electrons in the dot. Below, we will focus only on the first peak.

The first two (ground and first excited) α states contribute to this peak. Both are above resonance. The second and higher excited states are below resonance. Their contribution to T is very little. Thus, there are not channels at maximum resonance, and the value of T at the peak is lower than the maximum $T_2^{\text{res}} \sim 0.85$ for the $\alpha = 2$ channel. With a small decrease of V_g , T reaches the value T_2^{res} , meaning that there is one channel at maximum resonance. Notice that the distance between the first and second excited α states is only 0.12 meV. It means that only levels which are very close in energy may be simultaneously resonant. The width of the one-channel peak, ~ 0.05 meV, may serve as an estimation of the resonance interval.

The sensitivity of the first peak maximum with the number of levels in the resonance interval may be used for an experimental estimation of the density of levels at low excitation energies. We prove this statement in Fig. 4. The number of levels in an energy interval $\delta = 0.05$ meV below the excitation energy ΔE is drawn along with the estimate (points) obtained from the conductance in the following way.

We follow the first peak maximum for different V_g . Its position, i. e. the value of V_{sd} , is identified with the excitation energy ΔE , and from the height, T_{peak} , we obtain the number of levels in the resonance interval as

$$n = \ln(1 - T_{peak}) / \ln(1 - T_1^{res}), \quad (17)$$

where T_1^{res} is the value of T when the first excited state $\alpha = 1$ is at maximum resonance. The idea behind Eq. (17) is that the product in Eq. (16) may be approximated as $(1 - T_1^{res})^n$.

We compare in Figs. 4 (a) and (b) the estimation coming from Eq. (17) with the exact level distribution obtained before. The agreement is excellent. Abrupt variations of the density of levels are nicely reproduced as well as the smooth behaviour obtained from Eq. (3). This agreement proves the factibility of measuring the low-energy density of levels in few-electron quantum dots by means of a precise measurement of the conductance.

In conclusion, we have computed the density of spin-polarized levels of 6- and 7-electron quantum dots at low excitation energies and strong magnetic fields. The density is well parametrized by a constant temperature approximation. The temperature parameter, Θ , shows a weak dependence on the magnetic field. We computed also the dot conductance (transmission coefficient) for vertical tunneling, and showed that the conductance at the upper edge of the Coulomb blockade diamond is directly related to the density of levels. In this way, a procedure is suggested for the experimental determination of the low-lying density of states from a precise measurement of the conductance. Altough calculations were carried out under the simplifying assumptions of zero temperature and strong magnetic fields, extensions to zero or weak fields and finite temperatures are also possible.

ACKNOWLEDGMENTS

A. G. acknowledges the Research Committee of the University of Antioquia (CODI) for support.

^a Electronic address: agonzale@fisica.udea.edu.co

^b Electronic address: rcapote@infomed.sld.cu

¹ S. Tarucha in Mesoscopic Physics and Electronics, T. Ando, Y. Arakawa, K. Furuya et al (eds.), Springer, Berlin (1998), p. 66.

² S. Tarucha, D. G. Austing, and T. Honda, Phys. Rev. Lett. 77, 3613 (1996).

³ T. H. Oosterkamp, J. W. Janssen, L. P. Kouwenhoven et al, Phys. Rev. Lett. 82, 2931 (1999).

⁴ L. P. Kouwenhoven, T. H. Oosterkamp, M. W. S. Danoesastro et al, Science 278, 1788 (1997).

⁵ S. Sasaki, S. De Franceschi, J. M. Elzerman et al, Nature 405, 764 (2000).

⁶ S. De Franceschi, S. Sasaki, J. M. Elzerman et al, cond-mat/0007448. To appear in Phys. Rev. Lett.

⁷ The contribution of higher LL's to the low-lying density of states is currently under evaluation, J. D. Serna and A. Gonzalez, work in progress.

⁸ T. Ericson, Adv. Phys. 9, 425 (1960); A. Gilbert and A. G. W. Cameron, Can. J. Phys. 43, 1446 (1965).

⁹ T. Ando in Mesoscopic Physics and Electronics, T. Ando, Y. Arakawa, K. Furuya et al (eds.), Springer, Berlin (1998), p. 11.

¹⁰ L. Viña, J. Phys.: Condens. Matter 11, 5929 (1999).

¹¹ A. V. Khaetskii and Y. V. Nazarov, Phys. Rev. B 61, 12639 (2000).

¹² J. M. Blatt and V. F. Weisskopf, Theoretical Nuclear Physics, John Wiley and Sons, New York (1952), p. 401.

FIG. 1. (a) Schematic conduction band profile for the quantum dot under study. The magnetic field is aligned with the current along the z axis. (b) The $N=6$ Coulomb blockade diamond. We compute the conductance for a fixed V_g and varying V_{sd} , as represented by the dashed line.

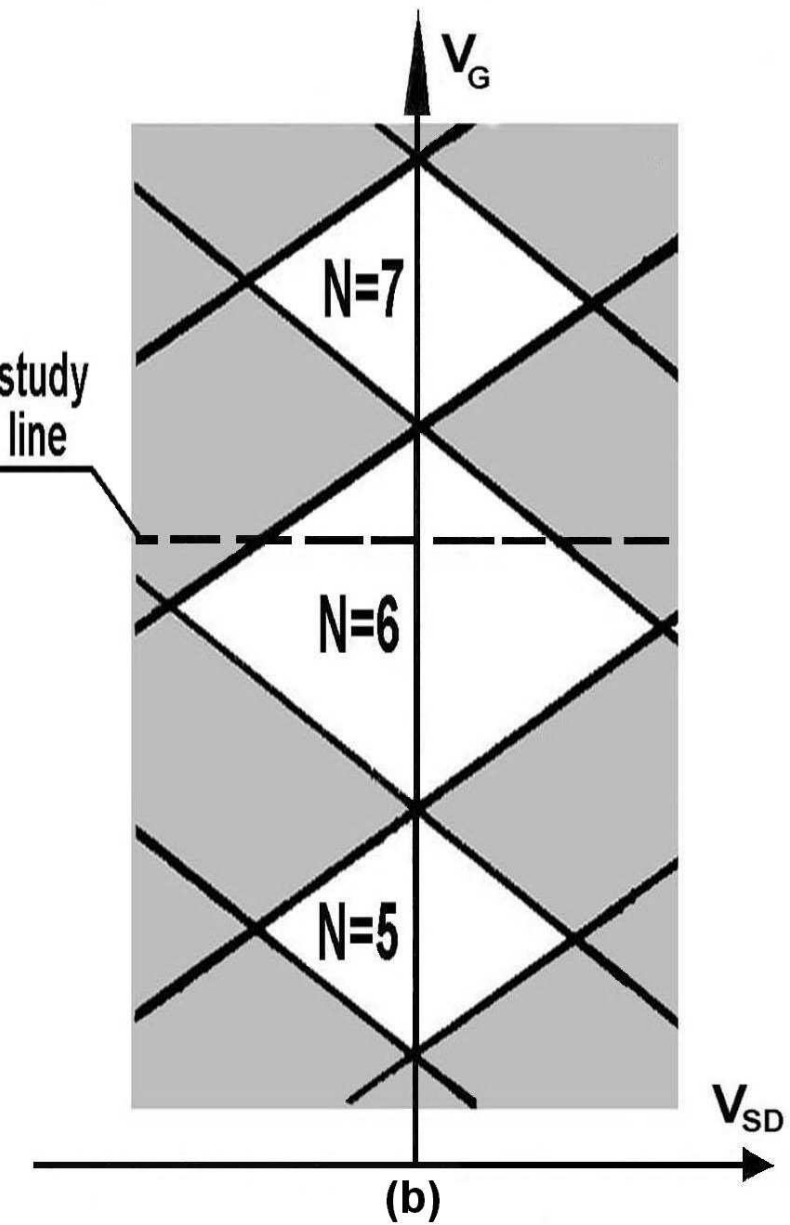
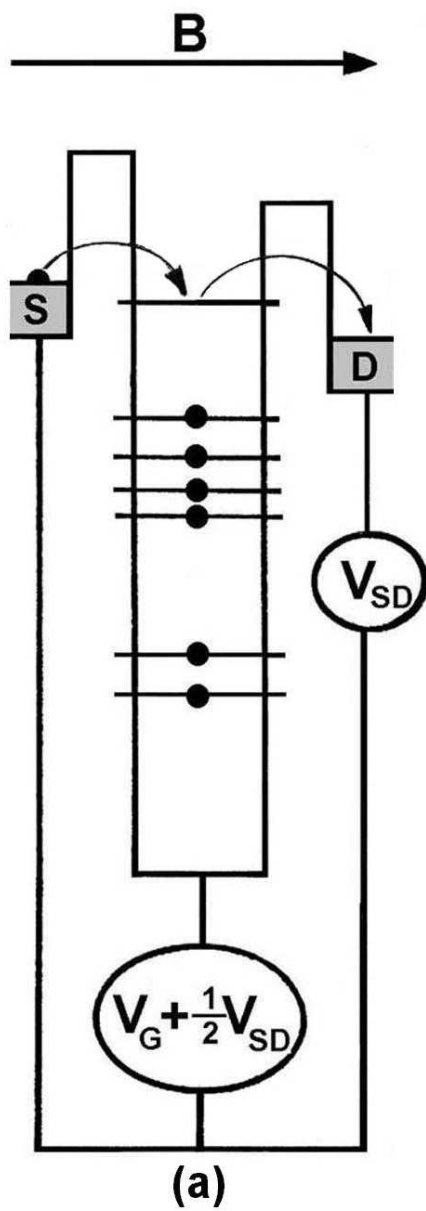
FIG. 2. The low-lying energy levels of the $N = 6$ and $N = 7$ dots at $B = 8.75$ and 12 T.

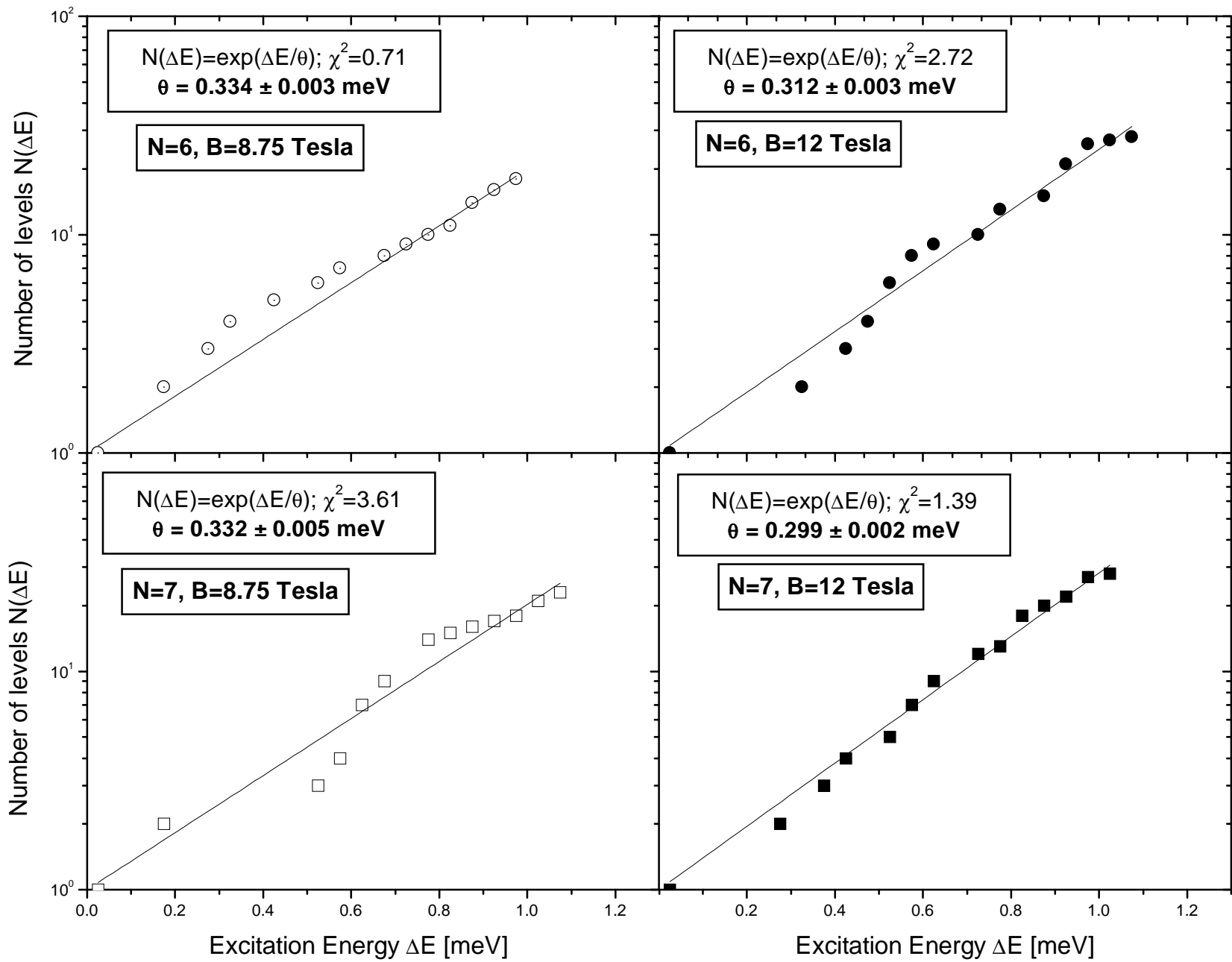
FIG. 3. (a) Partial transmission coefficient corresponding to the second excited (final) state at $B = 12$ T. (b) Total transmission at $V_g = 39.89$ meV and $B = 12$ T.

FIG. 4. Number of levels in the resonance interval $(\Delta E - \delta, \Delta E)$ with $\delta = 0.05$ meV. Exact results and the estimate coming from Eq. (17) are compared. (a) $B = 12$ T. (b) $B = 8.75$ T.

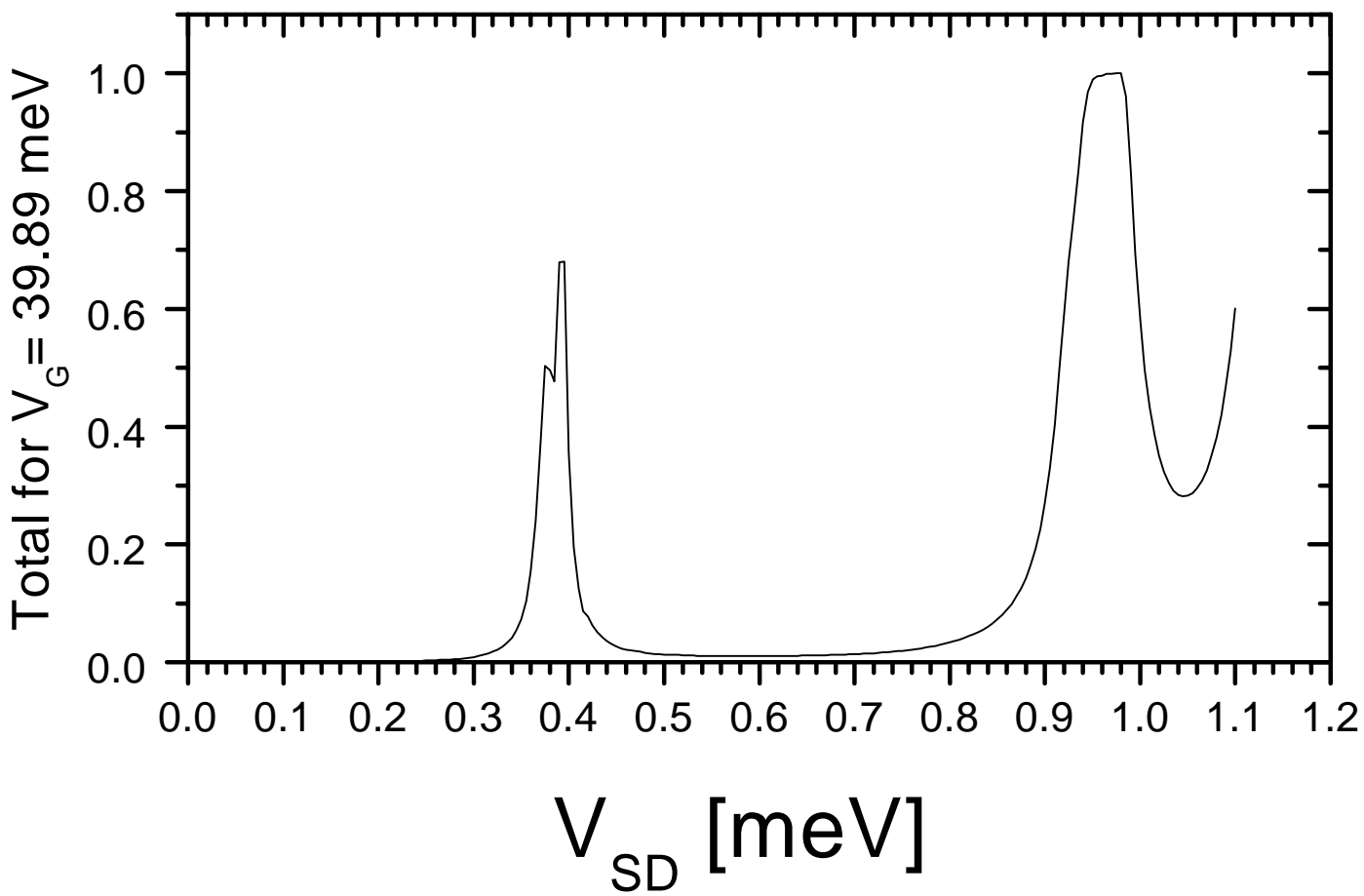
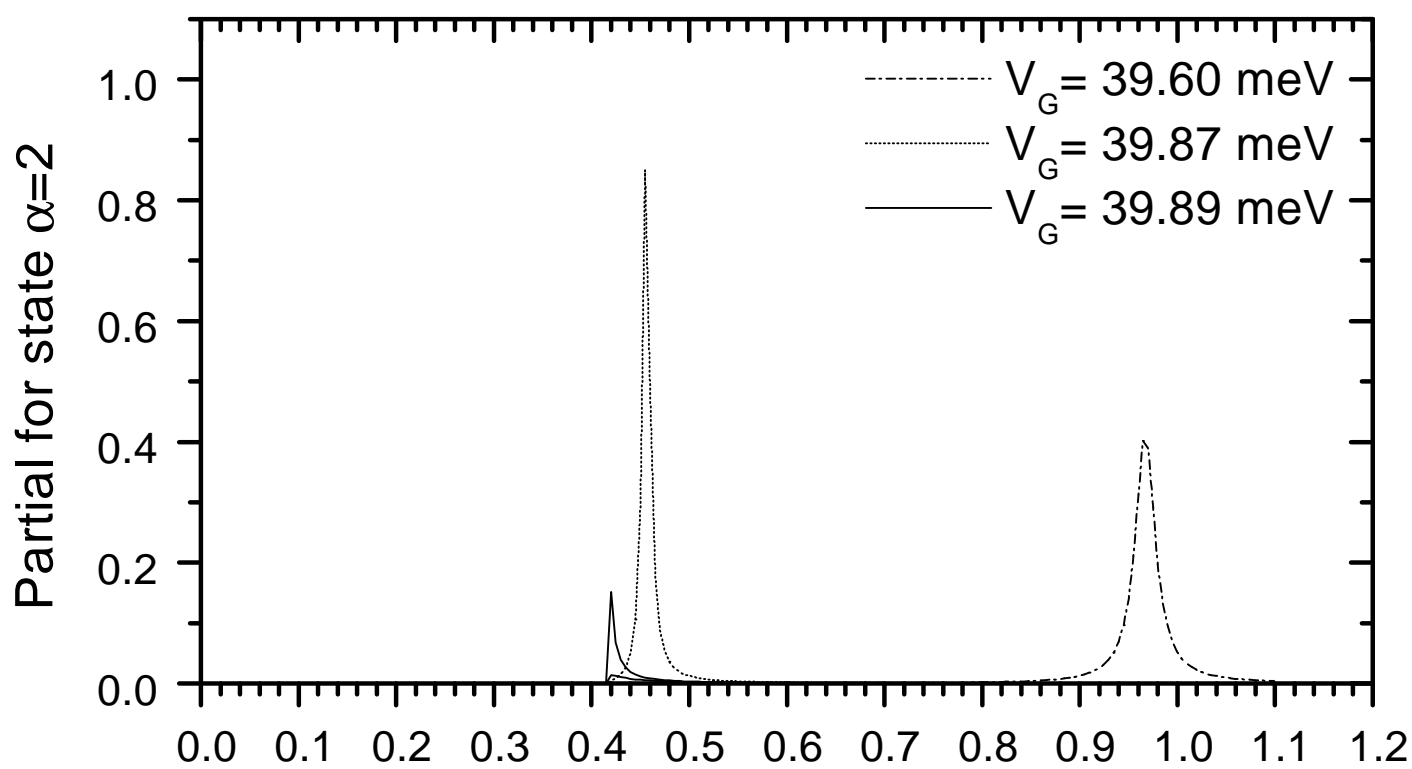
This figure "fig1.jpg" is available in "jpg" format from:

<http://arxiv.org/ps/cond-mat/0102030v1>





B=12 T
TRANSMISSION COEFFICIENTS



N=6

